PERGAMON

Available online at www.sciencedirect.com

SCIENCE DIRECT®

Engineering Fracture Mechanics 70 (2003) 2617–2624

Engineering Fracture Mechanics

www.elsevier.com/locate/engfracmech

Technical note

Fatigue threshold and crack growth in an electron beam weld made of steel and bronze

Michal Vorel [a,*], Milan Růžička [b]

[a] *Department of Engineering Design, Faculty of Mechanical Engineering and Process Technology, Technical University Chemnitz, Reichenhainer Street 70, 09126 Chemnitz, Germany*

[b] *Department of Mechanics, Faculty of Mechanical Engineering, Czech Technical University in Prague, Technická 4, 166 07 Prague, Czech Republic*

Received 15 November 2002; accepted 24 April 2003

Abstract

In this research topic some experimental tests with single-edge notched beams were performed to determine the threshold load value for fatigue crack growth and to characterize fatigue crack behaviour of an electron beam weld made of steel and bronze. Subsequently, numerical analyses were done to estimate the threshold value ΔK_{th} and to simulate the fatigue crack growth. The calculated crack path was compared to those determined experimentally. The objective was to find out the necessary fracture properties for an analysis of an electron beam welded worm wheel and to asses the capability of usual fracture analysis software to simulate fatigue crack growth in welds.

Keywords: Electron beam weld; Crack growth; Fracture; Threshold value; Numerical analysis

1. Introduction

Electron beam welded joints made of steel and bronze are commonly used in worm wheels consisting of a bronze rim and a steel hub or in large engine shafts with a thick bronze coating. In recent research works it has been shown, that under unsuitable conditions there can be widespread cracks directly in the middle of the weld [1]. However, it is still not known how the cracks behave under fatigue loading. Therefore, to be able to produce a safe design the knowledge of the threshold value ΔK_{th} is necessary. It is related to the maximum stress field at the crack tip, at which no fatigue crack growth initiates. In this paper experimental and numerical methods were used to estimate the threshold value in small electron beam welded standardized four-point single-edge bend (SENB) specimens according to [2] made of steel and bronze.

Fracture properties of mismatched welded joints made of different materials were already described in many papers [3–5]. Basic static analysis of a crack in an electron beam weld of two different steels was also reported [6]. Fatigue crack growth in arc and gas welded joints has been the focus of many experimental

* Corresponding author. Tel.: +49-371-531-4566; fax: +49-371-531-4560.
E-mail address: michal.vorel@mbv.tu-chemnitz.de (M. Vorel).

0013-7944/$ - see front matter © 2003 Elsevier Ltd. All rights reserved.
doi:10.1016/S0013-7944(03)00164-4

Nomenclature

a	crack length
m	Paris law exponent
B	specimen width
C	Paris law constant
E	Young's modulus
K	stress intensity factor (SIF)
K_c	fracture toughness
K_{max}	maximum stress intensity factor
K_{min}	minimum stress intensity factor
K_{th}	threshold for fatigue crack growth
K_v	effective stress intensity factor
K_I	stress intensity factor for mode I
K_{II}	stress intensity factor for mode II
$M_{R_{p0.2}}$	mismatch factor with respect to yield stresses
N	number of load cycles
R	stress ratio
R_e	proportional limit stress
$R_{p0.2}$	yield stress
v	Poisson's ratio
ϕ	crack propagation (kink) angle
Δ	alternating value, e.g. $\Delta K = K_{max} - K_{min}$

works [7–9]. Some proved fracture analysis procedures for mismatched welds were summarized in industrial standards and recommendations [10,11]. For numerical analysis of cracks specialized finite- or boundary-element programs can be used [12–14]. By using models with many material zones fracture analysis of cracks in welds is also possible. To determine stress intensity factors and crack extension direction usual numerical procedures are involved [15–17]. Despite extensive research in fracture mechanics being made, there is still no knowledge on how a crack behaves in a weld between severely different base materials, e.g. crack growth across the heat affected zones.

2. Test materials

Base materials of the weld were structural steel S355J2 and tin bronze CC484K. They were welded in a form of two small rectangular bars in order to keep residual stresses at minimum. No heat treatment was done so that the welded joint was closely similar to the one of the worm wheel. In a cross cut the weld was completely free of inclusions and cracks. Whereas the heat affected zone (HAZ) of steel was clearly visible, the HAZ of bronze could be only roughly defined on the grounds of minor changes in the grain structure. The stress–strain curves of the base materials and of the weld metal were already known [18,19]. Tensile tests of the both HAZ were performed with mini tensile specimens [1]. Concluding from the yield stresses of the weld material (wm) the joint is slightly overmatched with respect to bronze (bz),

$$M_{R_{p0.2}} = \frac{R_{p0.2}^{wm}}{R_{p0.2}^{bz}} = 1.5 \tag{1}$$

Table 1
Material properties of an electron beam weld (see also [19])

Material zone	Thickness (mm)	E-module (GPa)	$R_{p0.2}$ (MPa)	R_m (MPa)	$M_{R_{p0.2}}$	
					Steel	Bronze
Steel *S355J2*	–	200	307	450	–	–
HAZ steel	0.8	200	630	810	2.1	–
Weld material	1.2	130	318	325	1.0	1.5
HAZ bronze	1.0	70	260	310	–	1.2
Bronze *CC484K*	–	110	212	325	–	–

and almost evenmatched with respect to steel (st, see also Table 1),

$$M_{R_{p0.2}} = \frac{R^{wm}_{p0.2}}{R^{st}_{p0.2}} = 1.0 \tag{2}$$

This means, that the strain field at the crack tip will be deformed to the side of bronze and that the crack should grow in the bronze base metal.

3. Experimental investigation of the threshold load

In welded parts the threshold value of effective stress intensity factor (SIF) at the onset of fatigue crack growth can only be determined indirectly. Because of the mismatch effect merely the threshold load can experimentally be investigated and using this the appropriate SIF can then be calculated. To this end, two SENB specimens were used in the experiments (Fig. 1). In the weldment they were oriented with their longitudinal axis perpendicular to the welding beam advance direction. The notch was eroded with a 200 μm wire directly in the middle of the weld material. Due to very small loading forces the experiments were conducted on a MTS Minibionix test machine with a 500N force transducer. The crack growth was measured visually with a fine eyepiece scale of a special Carl Zeiss microscope. The crack was extended by fatigue loading to a length of 0.1–0.2 mm. After that, the test method for determination of threshold load presented in [20] was used (Fig. 2). This is based on a stepwise increase of the loading amplitude from little values while observing the crack tip. If it starts moving, the loading amplitude must be decreased and the procedure is repeated with smaller steps. The threshold load amplitudes were therefore determined as intervals of two values (Table 2). A stress ratio $R = 0.1$ was used. Due to small ligament length, the load

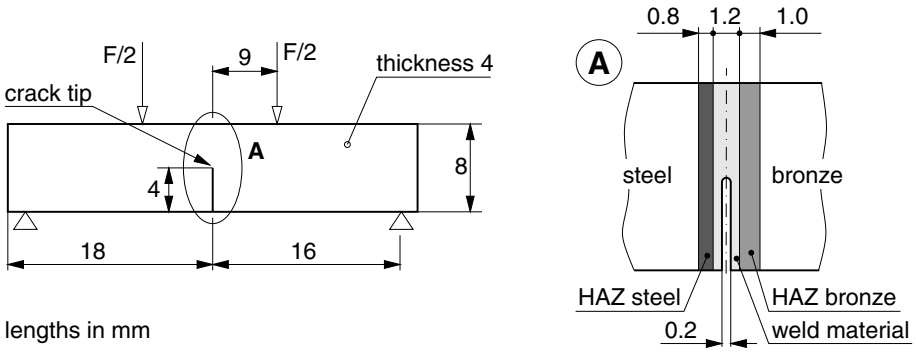

Fig. 1. Measures of the used SENB specimen.

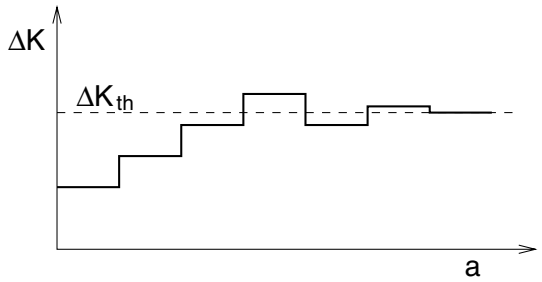

Fig. 2. Test method for the determination of the threshold load after [20].

Table 2
Specimens with crack lengths, loading amplitudes and their states

Specimen	Crack length a (mm)	Loading amplitude F_{th} (N)	State
1	0.74	138	Growing
	0.74	125	Arrested
2	0.56	144	Growing
	0.35	140	Arrested

shedding procedure after [21] could not have been used. On the one hand it would allow elimination of crack closure effects, but on the other hand crack extension to bigger lengths would be necessary. After finding the lowest loading amplitude for the crack growth, the experiment was carried at a slightly elevated loading to investigate the fatigue crack growth until an unstable crack growth began. This also revealed the structure of the crack surfaces (Fig. 3). During the stable crack growth the crack remained always within the weld metal but it diverted gradually from the original straight direction towards the HAZ bronze. The onset of the unstable crack growth took place shortly before the moving crack tip reached the interface between the weld metal and the HAZ bronze. The crack surfaces showed some plastic deformations in the HAZ bronze.

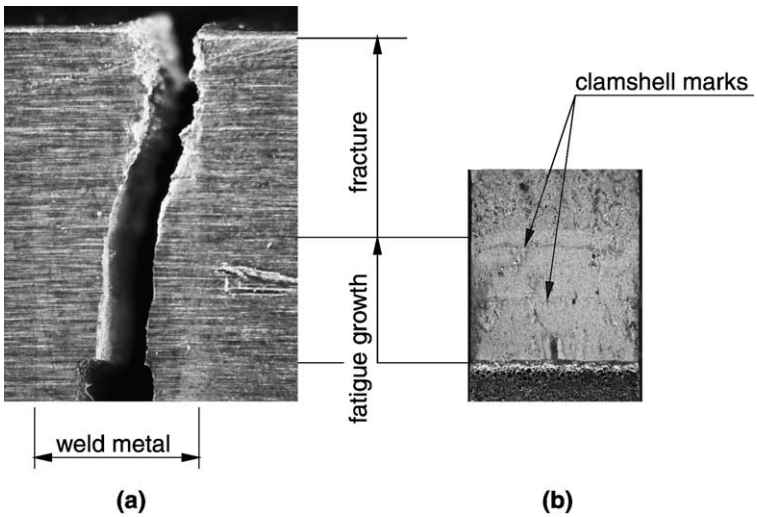

Fig. 3. Crack path (a) and crack surface (b) of a welded SENB specimen.

4. Numerical determination of ΔK_{th}

With heterogeneous materials stress intensity factors cannot be determined with usual formulas. The only feasible way is the use of numerical methods, such as the finite-element analysis. For the purpose of this research work the FE-program Franc/FAM proved most suitable [12]. It allows elastic plain strain, plain stress or axysymmetric analyses, although solving simple plastic problems is also possible. The crack geometry can have an arbitrary two-dimensional form. The software enables crack growth simulation through many material zones, while using several methods for the calculation of stress intensity factors and for the determination of the crack growth direction. The basic function of the program is shown in Fig. 4. For the purpose of this study a five zone model (steel, HAZ steel, weld metal, HAZ bronze, broze) was defined with linear elastic material properties. The notch was defined as a sharp initial crack in the middle of the weld metal (Fig. 5). To determine the SIF the modified virtual crack closure method was used [15]. The effective SIF was determined with the method suggested by Richard [12]:

$$K_v = \frac{K_I}{2} + \frac{1}{2}\sqrt{K_I^2 + 4(\alpha K_{II})^2}, \quad \alpha = 1.15 \tag{3}$$

The crack was manually extended after the observation of the crack path geometry in the test specimens. When the crack length corresponded to that of the threshold load amplitude (see Table 2) the threshold value was determined as the effective SIF (Table 3). This was justified stating that the conditions

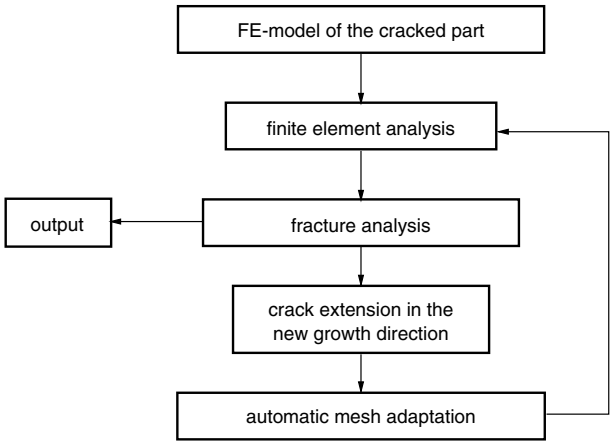

Fig. 4. Basic function of the program Franc/FAM.

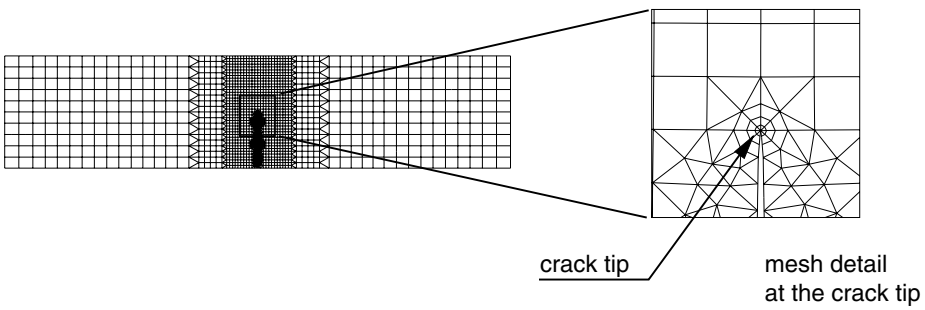

Fig. 5. FE mesh of the SENB model.

Table 3
Numerically determined stress intensity factors

Specimen	K_I (MPa m$^{1/2}$)	K_{II} (MPa m$^{1/2}$)	$K_v = K_{th}$ (MPa m$^{1/2}$)
1	5.3	0.6	5.3
	4.8	0.5	4.8
2	5.1	0.5	5.1
	4.6	0.5	4.6
Average			4.9

$$B \geqslant 2.5\left(\frac{K_v}{R_{p0.2}}\right)^2 \quad \text{and} \quad r_{pl} = \frac{1}{2\pi}\left(\frac{K_v}{R_e}\right)^2(1-2v) \tag{4}$$

remained valid. The calculated threshold value is somewhat lower than that of steel (for S355J2 $\Delta K_{th} = 5.9$ MPa m$^{1/2}$) and it remains much lower than the fracture toughness of the weld metal (based on some preliminary experiments $K_c \approx 54$ MPa m$^{1/2}$). Smaller threshold value of the weld metal may be caused by some soft copper phases found in a metallographic analysis of the weld. The approximate models, e.g. after [22]:

$$\Delta K_{th} = 1.12\text{–}1.73 \times 10^{-5}E \tag{5}$$

gives threshold values lower then 2.3 MPa m$^{1/2}$. However, such models were developed for homogeneous materials with completely different microstructure and they may not be appropriate in this study.

5. Simulation of crack growth

Simulation of the crack growth from the initial crack length was also performed. For this purpose the Erdogan–Ratwani [23] crack growth model

$$\frac{da}{dN} = \frac{C(\Delta K - \Delta K_{th})^m}{(1-R)(K_c - K_{max})} \tag{6}$$

and the method after Richard [12] for the determination of the kink angle

$$\phi = \mp\left[2.714\frac{K_{II}}{K_I + K_{II}} - 1.456\left(\frac{K_{II}}{K_I + K_{II}}\right)^2\right] \tag{7}$$

were used. The simulation was performed on a similar model with a sharp initial crack as in Section 4. The calculated crack path differs from the one determined experimentally (Fig. 6). This can be caused by an inappropriate material properties of the model. The course of hardness across the weld showed that there is a small decrease in hardness within the weld metal [1], which means that there are further changes of the material properties within the weld. If those were considered in the numerical model as fine regions within the weld metal, a more precise stress field would be calculated. As a result the direction angles would be different and possibly a more accurate crack path could be determined. However, it would also be possible to develop special crack growth model, that corrects the direction angles in dependence on the distance from the weld center. Such a model would be applicable only to this specific weld joint and would no more be independent of the material properties.

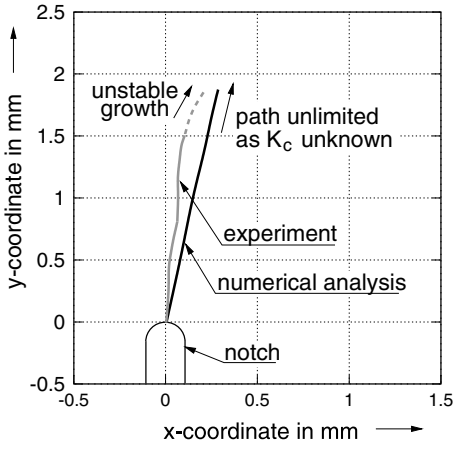

Fig. 6. Comparison of the experimentally and numerically determined crack paths.

6. Conclusion

In this paper investigations of the threshold value ΔK_{th} for a fatigue crack growth in an electron beam welded joint of steel and bronze were performed. For this purpose experimental methods to determine the threshold load and numerical methods to analyze the stress intensity factors were used. The calculated threshold value is somewhat lower than that of steel. In order to verify a numerical model for the fatigue crack growth, a crack extension in the weld metal was simulated. The calculated crack path differs from that determined experimentally. This may be caused by insufficient knowledge of the material properties of the weld metal, although special mini tensile specimens to determine the stress–strain curves were used. Therefore, more extensive experiments are planned in order to clarify the differences between the real crack path and the one determined numerically. The determined threshold value will be used for a fracture analysis of an electron beam welded worm wheel made of a steel hub and a bronze rim.

References

[1] Vorel M, Leidich E. Impact of residual stresses on crack distribution in an electron beam welded worm wheel. In: Maschinenbau und Nanotechnik, 47. Internationales Wissenschaftliches Kolloquium, Ilmenau, 2002.
[2] ASTM E399-90. Standard Test Method for Plane-Strain Fracture Toughness of Metallic Materials.
[3] Eripret C, Hornet P. Mis-matching of welds. In: Prediction of overmatching effects on the fracture of stainless steel cracked welds. London: ESIS, Mechanical Engineering Publications; 1994. p. 685–708.
[4] Koçak M, Kim Y, Hornet P. Recommendations for J and CTOD testing of strength mis-match weldments: GKSS and EDF view. Weld mis-match effect. Technical report, GKSS, 1997.
[5] Kim YJ, Schwalbe KH. Mismatch effect on plastic yield loads in idealised weldments: I. Weld centre cracks. Engng Fract Mech 2001;68:163–82.
[6] Buddenberg T, Riekehr S, Kim J-Y, Koçak M. Der einfluss des festigkeits-mis-matchs auf das bruchverhalten von elektronenstrahlschweißnähten. Technical Report DVS 187, DVS, 1998.
[7] Hidvéghy J, Buršák M, Michel J. Fatigue crack growth in welds of high strength microalloyed steel. Metalurgija 1999;38:19–23.
[8] Ohta A. Evaluation of fatigue crack growth in welded joints. In: NRIM research activities. NRIM; 1994.
[9] Cheng G, Kuang B, Lou ZW, Li H. Experimental investigation of fatigue behaviour for welded joint with chemical heterogenity. Int J Pres Ves Pip 1996;67:229–42.
[10] Schwalbe KH, Kim YJ, Hao S, Cornec A, Koçak M. EFAM ETM-MM 96. The ETM method for assessing the significance of crack-like defects in joints with mechanical heterogeneity (strength mismatch). Ergebnissbericht GKSS 97/E/9, GKSS Forschungszentrum Geesthacht, 1997.

[11] Berger C, Blauel JG, Hodulak L, Wurm B, editors. Bruchmechanischer Festigkeitsnachweis für Maschinenbauteile. FKM-Richtlinie für den bruchmechanischen Festigkeitsnachweis. VDMA Verlag, Frankfurt am Main, 1. edition, 2001.
[12] Schöllman M, Richard HA. Franc/FAM—a software for the prediction of crack propagation. J Struct Engng 1999;26:39–48.
[13] Timbrell C, Cook G. 3d FE fracture mechanics analysis for industrial applications. In: Inelastic Finite Element Analysis, Institute of Mechanical Engineers, London, 1997.
[14] Franc3d: a three dimensional fracture analysis code, Version 1.14, Cornell University, New York, 1998.
[15] Rybicky EF, Kanninen MF. A finite element calculation of stress intensity factors by modified crack closure integral. Engng Fract Mech 1977;9:931–8.
[16] Barsoum RS. On the use of isoparametric finite elements in linear fracture mechanics. Int J Numer Methods Engng 1976;10:25–37.
[17] Vorel M, Leidich E. Accuracy of determining stress intensity factors in some numerical programs. Acta Polytech 2001;41:60–6.
[18] Engineering-e.com. Material Database. WWW-page, http://www.engineering-e.com/, last change: 04.11.2002, accessed: 06.11.2003, 11:15GMT.
[19] Schmidt G. Untersuchungen zur Tragfähigkeit elektronenstrahlgeschweisster Schneckenräder. Berichte aus dem Maschinenbau. Shaker Verlag, Aachen, 1. edition, 1999.
[20] Klesnil M, Lukas P. Influence of strength and stress history on growth and stabilization of fatigue cracks. Engng Fract Mech 1972;4:77–92.
[21] ASTM E647-91. Standard test method for measurement of fatigue crack growth rates.
[22] DVS Merkblatt 2401-1987. Bruchmechanische Bewertung von Fehlern in Schweissverbindungen.
[23] Erdogan F, Ratwani M. Fatigue and fracture of cylindrical shells containing a circumferential crack. Int J Fract Mech 1970;6:379–92.